

# Caspase inhibitor decreases apoptosis in pyrogallol-treated lung cancer Calu-6 cells via the prevention of GSH depletion

YONG HWAN HAN, SUHN HEE KIM, SUNG ZOO KIM and WOO HYUN PARK

Department of Physiology, Medical School, Institute for Medical Sciences, Centers for Healthcare Technology Development, Chonbuk National University, JeonJu 561-180, Korea

Received July 3, 2008; Accepted August 18, 2008

DOI: 10.3892/ijo\_00000099

**Abstract.** Pyrogallol (PG) is a polyphenol compound and is known to be an  $O_2^-$  generator. In the present study, we evaluated the anti-apoptotic effects of caspase inhibitors in relation to changes in reactive oxygen species (ROS) and glutathione (GSH) levels in PG-treated human pulmonary adenocarcinoma Calu-6 cells. Treatment with 50  $\mu$ M PG inhibited the growth of Calu-6 cells ~60% and induced apoptosis ~17% at 24 h, accompanied by mitochondrial membrane potential loss ( $\Delta\Psi_m$ ). Treatment with pan-caspase inhibitor (Z-VAD-FMK), caspase-3 inhibitor (Z-DEVD-FMK), caspase-8 inhibitor (Z-IETD-FMK) and caspase-9 inhibitor (Z-LEHD-FMK) significantly prevented apoptosis in PG-treated Calu-6 cells at 24 h. PG increased the ROS and depleted GSH contents in Calu-6 cells. Treatment with each caspase inhibitor did not significantly change the ROS and GSH levels in PG-treated Calu-6 cells at 24 h. However, Z-VAD significantly prevented GSH depletion in PG-treated Calu-6 cells at the late time phase of 72 h. Conclusively, the anti-apoptotic effect of caspase inhibitor on PG-induced Calu-6 cell death was closely related to changes in GSH content rather than ROS levels.

## Introduction

The mechanism of apoptosis mainly involves two signaling pathways, the mitochondrial and cell death receptor pathways (1-3). The key element in the mitochondrial pathway is the efflux of cytochrome *c* from mitochondria to cytosol, where it subsequently forms a complex (apoptosome) with Apaf-1 and caspase-9, leading to the activation of caspase-3 (4). The cell death receptor pathway is characterized by the binding of cell death ligands and cell death receptors, and subsequently activates caspase-8 and -3 (5,6). Caspase-3 is an executioner caspase, whose activation can systematically dismantle cells by cleaving key proteins such as PARP.

Pyrogallol (PG) is a polyphenol compound and is known to be a superoxide anion ( $O_2^-$ ) generator (7,8). This compound is often used to investigate the role of  $O_2^-$  in the biological system. The superoxide anion ( $O_2^-$ ) belongs to the reactive oxygen species (ROS) including hydrogen peroxide ( $H_2O_2$ ), hydroxyl radical ( $OH$ ) and peroxynitrite ( $ONOO^-$ ). These ROS have recently been implicated in the regulation of many important cellular events, including transcription factor activation, gene expression, differentiation and cell proliferation (9-11). ROS are formed as by-products of mitochondrial respiration or certain oxidases such as nicotine adenine diphosphate (NADPH) oxidase, xanthine oxidase (XO), and a number of arachidonic acid oxygenases (12). A change in the redox state of tissue implies a change in the generation or metabolism of ROS. Principal metabolic pathways include superoxide dismutase (SOD), which is expressed as extracellular, intracellular and mitochondrial isoforms (13). These isoforms metabolize  $O_2^-$  to  $H_2O_2$ . Further metabolism by peroxidases which include catalase and glutathione (GSH) peroxidase yields  $O_2$  and  $H_2O$  (14). Cells possess antioxidant systems to control the redox state, which is important for their survival. Excessive production of ROS gives rise to the activation of events that lead to death in several cell types (15-18). Also, PG was shown to induce  $O_2^-$ -mediated death of several types of cells such as mesangial (19), human lymphoma (7), human glioma (20) and As4.1 juxtaglomerular cells (21). The exact mechanisms involved in cell death induced by ROS are not fully understood.

Lung cancer is a major cause of cancer-related death in developed countries. Various novel therapeutic strategies are

---

*Correspondence to:* Dr Woo Hyun Park, Department of Physiology, Medical School, Institute for Medical Sciences, Centers for Healthcare Technology Development, Chonbuk National University, JeonJu 561-180, Korea  
E-mail: parkwh71@chonbuk.ac.kr

**Abbreviations:** PG, pyrogallol; ROS, reactive oxygen species; SOD, superoxide dismutase; FBS, fetal bovine serum; MTT, 3-(4,5-dimethylthiazol-2-yl)-2,5-diphenyltetrazolium bromide; PI, propidium iodide; FITC, fluorescein isothiocyanate;  $H_2DCFDA$ , 2',7'-dichlorodihydrofluorescein diacetate; DHE, dihydroethidium; GSH, glutathione; CMFDA, 5-chloromethylfluorescein diacetate; HPF, 3'-(p-hydroxyphenyl) fluorescein; MMP, mitochondrial membrane potential

**Key words:** pyrogallol, apoptosis, Calu-6, caspase, reactive oxygen species

currently under consideration, as the clinical use of cytotoxic drugs is limited due to intrinsic or acquired resistance and toxicity (22). Studies of the molecular mechanisms of cytotoxic drug action have shed light on the treatment of lung cancer, and novel agents that target specific intracellular pathways related to the distinctive properties of cancer cells continue to be developed. However, little is known about the relationship between PG and lung cancer cells.

In the present study, we evaluated the anti-apoptotic effects of caspase inhibitors in PG-treated human pulmonary adenocarcinoma Calu-6 cells in relation to changes in ROS and GSH levels.

## Materials and methods

**Cell culture.** The human pulmonary adenocarcinoma Calu-6 cell line was obtained from the ATCC (HTB56) and was maintained in a humidified incubator containing 5% CO<sub>2</sub> at 37°C. Calu-6 cells were cultured in RPMI-1640 supplemented with 10% fetal bovine serum (FBS) and 1% penicillin-streptomycin (Gibco BRL, Grand Island, NY). Cells were routinely grown in 100-mm plastic tissue culture dishes (Nunc, Roskilde, Denmark) and harvested with a solution of trypsin-EDTA while in a logarithmic phase of growth. Cells were maintained in these culture conditions for all experiments.

**Reagents.** PG was purchased from Sigma-Aldrich Chemical Co. (St. Louis, MO). PG was dissolved in H<sub>2</sub>O at 1x10<sup>-1</sup> M as a stock solution. Pan-caspase inhibitor (Z-VAD-FMK; benzyloxycarbonyl-Val-Ala-Asp-fluoromethylketone), caspase-3 inhibitor (Z-DEVD-FMK; benzyloxycarbonyl-Asp-Glu-Val-Asp-fluoromethylketone), caspase-8 inhibitor (Z-IETD-FMK; benzyloxycarbonyl-Ile-Glu-Thr-Asp-fluoromethylketone) and caspase-9 inhibitor (Z-LEHD-FMK; benzyloxycarbonyl-Leu-Glu-His-Asp-fluoromethylketone) were obtained from R&D Systems, Inc. (Minneapolis, MN) and were dissolved in dimethyl sulfoxide (DMSO) (Sigma) at 1x10<sup>-2</sup> M as a stock solution, which also was used as a control vehicle. All of the stock solutions were wrapped in foil and kept at 4 or -20°C.

**Cell growth inhibition assay.** The *in vitro* cell growth inhibition effect of PG on Calu-6 cells was determined by measuring 3-(4,5-dimethylthiazol-2-yl)-2,5-diphenyl-tetrazolium bromide (MTT) dye absorbance of living cells as described previously (23). In brief, 5x10<sup>4</sup> cells per well were seeded in 96-well microtiter plates (Nunc, Roskilde, Denmark) in the presence of 50 μM PG following 1 h of pre-incubation with 12.5 μM caspase inhibitor. After exposure to PG for 24 h, 50 μl of MTT (Sigma) solution (2 mg/ml in PBS) was added to each well, and the plates were incubated for an additional 3 h at 37°C. MTT solution in medium was aspirated off. To achieve solubilization of the formazan crystals formed in viable cells, 200 μl of DMSO was added to each well. The optical density of each well was measured at 570 nm using a microplate reader (Spectra Max 340, Molecular Devices Co, Sunnyvale, CA, USA). Each plate contained multiple wells at a given experimental condition and multiple control wells.

**Annexin V staining.** Apoptosis was determined by staining cells with Annexin V-fluorescein isothiocyanate (FITC) (Ex/Em = 488 nm/519 nm), because Annexin V can be used to identify the externalization of phosphatidylserine during the progression of apoptosis and, therefore, can detect cells during early phases of apoptosis. In brief, 1x10<sup>6</sup> cells were incubated with 50 μM PG after 1 h of pre-incubation with 12.5 μM caspase inhibitor for 24 or 72 h. Cells were washed twice with cold PBS and then resuspended in 500 μl of binding buffer (10 mM HEPES/NaOH pH 7.4, 140 mM NaCl, 2.5 mM CaCl<sub>2</sub>) at a concentration of 1x10<sup>6</sup> cells/ml. Annexin V-FITC (5 μl; Pharmingen, San Diego, CA) was then added to these cells, which were analyzed with a FACStar flow cytometer (Becton Dickinson). For each sample, 5,000 or 10,000 events were collected.

**Measurement of mitochondrial membrane potential (MMP) ( $\Delta\Psi_m$ ).** The mitochondrial membrane was monitored using the Rhodamine 123 fluorescent dye (Ex/Em = 485 nm/535 nm), a cell-permeable cationic dye, which preferentially enters mitochondria based on the highly negative MMP ( $\Delta\Psi_m$ ). Depolarization of MMP ( $\Delta\Psi_m$ ) results in the loss of Rhodamine 123 from the mitochondria and a decrease in intracellular fluorescence. In brief, 1x10<sup>6</sup> cells were incubated with 50 μM PG after 1 h of pre-incubation with 12.5 μM caspase inhibitor for 24 or 72 h. Cells were washed twice with PBS and incubated with Rhodamine 123 (0.1 μg/ml; Sigma) at 37°C for 30 min. Rhodamine 123 staining intensity was determined by flow cytometry. For each sample, 5,000 or 10,000 events were collected.

**Detection of intracellular general ROS and O<sub>2</sub><sup>-</sup> concentration.** Intracellular general ROS such as H<sub>2</sub>O<sub>2</sub>, OH and ONOO were detected by means of an oxidation-sensitive fluorescent probe dye, 2',7'-dichlorodihydrofluorescein diacetate (H<sub>2</sub>DCFDA) or 3'-(p-hydroxyphenyl) fluorescein (HPF) (24) (Invitrogen Molecular Probes, Eugene, OR). H<sub>2</sub>DCFDA was deacetylated intracellularly by nonspecific esterase, which was further oxidized by cellular peroxides, yielding 2,7-dichloro-fluorescein (DCF), a fluorescent compound (Ex/Em = 495 nm/529 nm). HPF specifically reacts with OH and ONOO and yields a bright green fluorescent product (Ex/Em = 490 nm/515 nm). DCF and HPF are poorly selective for the superoxide anion radical (O<sub>2</sub><sup>-</sup>). In contrast, dihydroethidium (DHE) (Ex/Em = 518 nm/605 nm) (Invitrogen Molecular Probes) is a fluorogenic probe that is highly selective for O<sub>2</sub><sup>-</sup> among ROS. DHE is cell-permeable and reacts with the superoxide anion to form ethidium, which in turn intercalates in deoxyribonucleic acid, thereby exhibiting a red fluorescence. In brief, 1x10<sup>6</sup> cells were incubated with 50 μM PG after 1 h of pre-incubation with 12.5 μM caspase inhibitor for 24 or 72 h. Cells were then washed in PBS and incubated with 20 μM H<sub>2</sub>DCFDA, HPF or DHE at 37°C for 30 min according to the manufacturer's instructions. DCF, HPF and DHE fluorescences were detected using a FACStar flow cytometer. For each sample, 5,000 or 10,000 events were collected. ROS and O<sub>2</sub><sup>-</sup> levels were expressed as mean fluorescence intensity (MFI), which was calculated by CellQuest software.

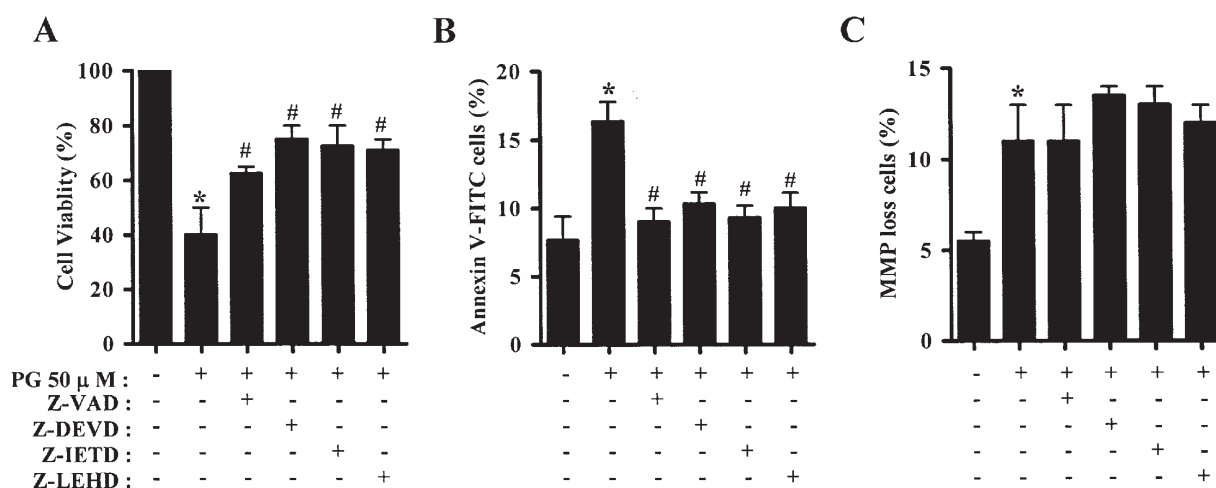


Figure 1. Effects of caspase inhibitors on cell growth, apoptosis and mitochondrial membrane potential (MMP) loss in PG-treated Calu-6 cells. Exponentially growing cells were treated with 50  $\mu$ M PG for 24 h following a 1-h pre-incubation with 12.5  $\mu$ M caspase inhibitor. (A) The growth of Calu-6 cells was assessed by an MTT assay. (B) Cells with Annexin V staining were counted using a FACStar flow cytometer. The graph shows the percentages of Annexin V-positive cells. (C) Cells stained with Rhodamine 123 were counted using a FACStar flow cytometer. The graph shows the percentages of Rhodamine 123-negative (MMP loss) cells. \*P<0.05 compared with the PG-untreated control group; #P<0.05 compared with cells treated with only PG.

**Detection of mitochondrial  $O_2^-$  concentration.** Mitochondrial  $O_2^-$  levels were detected by means of MitoSox<sup>TM</sup> Red mitochondrial  $O_2^-$  indicator (Invitrogen Molecular Probes), which is a fluorogenic dye for highly selective detection of  $O_2^-$  in the mitochondria of live cells. Once in the mitochondria, MitoSox Red agent is oxidized by  $O_2^-$  and exhibits red fluorescence (Ex/Em = 510 nm/580 nm). In brief,  $1 \times 10^6$  cells were incubated with 50  $\mu$ M PG after 1 h of pre-incubation with 12.5  $\mu$ M caspase inhibitor for 24 h. Cells were then washed in PBS and incubated with 5  $\mu$ M MitoSox Red agent at 37°C for 30 min according to the manufacturer's instructions. MitoSox Red fluorescence was detected using a FACStar flow cytometer. For each sample, 5,000 or 10,000 events were collected. MitoSox Red levels were expressed as mean fluorescence intensity (MFI), which was calculated by CellQuest software.

**Detection of intracellular glutathione (GSH).** Cellular GSH levels were analyzed using 5-chloromethylfluorescein diacetate (CMFDA, Molecular Probes) (Ex/Em = 522 nm/595 nm). CMFDA is a useful, membrane-permeable dye for determining levels of intracellular glutathione (25,26). In brief,  $1 \times 10^6$  cells were incubated with 50  $\mu$ M PG after 1 h of pre-incubation with 12.5  $\mu$ M caspase inhibitor for 24 or 72 h. Cells were then washed with PBS and incubated with 5  $\mu$ M CMFDA at 37°C for 30 min according to the manufacturer's instructions. Cytoplasmic esterases convert nonfluorescent CMFDA to fluorescent 5-chloromethylfluorescein, which can then react with glutathione. PI (1  $\mu$ g/ml), which is membrane impermeant and generally excluded from viable cells, was subsequently added, and CMF fluorescence and PI staining intensity were determined using a FACStar flow cytometer and calculated by CellQuest software. For each sample, 5,000 or 10,000 events were collected.

**Statistical analysis.** Results shown in the figures represent the mean of at least three independent experiments; bar, SD.

Microsoft Excel or Instat Software (GraphPad Prism4, San Diego, CA) was used to analyze the data. The Student's t-test or one-way analysis of variance (ANOVA) with *post hoc* analysis using Tukey's multiple comparison test was used for parametric data. Statistical significance was defined as P<0.05.

## Results

**Effects of caspase inhibitors on cell growth, apoptosis and mitochondrial membrane potential (MMP) loss in PG-treated Calu-6 cells at 24 h.** We examined the effect of caspase inhibitors on the growth of PG-treated Calu-6 cells using an MTT assay. We screened the range concentration of PG for this experiment and chose the suitable dose of 50  $\mu$ M PG, which inhibited the growth of Calu-6 cells ~60% at 24 h (Fig. 1A). We also determined 12.5  $\mu$ M to be the optimal dose of pan-caspase inhibitor (Z-VAD-FMK), caspase-3 inhibitor (Z-DEVD-FMK), caspase-8 inhibitor (Z-IETD-FMK) and caspase-9 inhibitor (Z-LEHD-FMK), which did not affect the growth of Calu-6 control cells (data not shown). Treatment with each caspase inhibitor significantly prevented the growth inhibition of Calu-6 cells by PG at 24 h (Fig. 1A). Each caspase inhibitor also rescued Calu-6 cells from PG-induced apoptosis at 24 h in view of Annexin V-positive staining (Fig. 1B), which indicated that the cell death of Calu-6 cells by PG occurred via an apoptotic pathway. It is known that apoptosis is closely related to the collapse of MMP ( $\Delta\Psi_m$ ) (27). Therefore, we determined the loss of MMP ( $\Delta\Psi_m$ ) in PG-treated Calu-6 cells. As expected, the loss of MMP ( $\Delta\Psi_m$ ) was observed in PG-treated cells at 24 h (Fig. 1C). However, treatment with each caspase inhibitor did not significantly change the levels of MMP loss ( $\Delta\Psi_m$ ) in PG-treated cells at this time (Fig. 1C).

**Effects of caspase inhibitors on ROS and GSH levels in PG-treated Calu-6 cells at 24 h.** To determine whether the levels

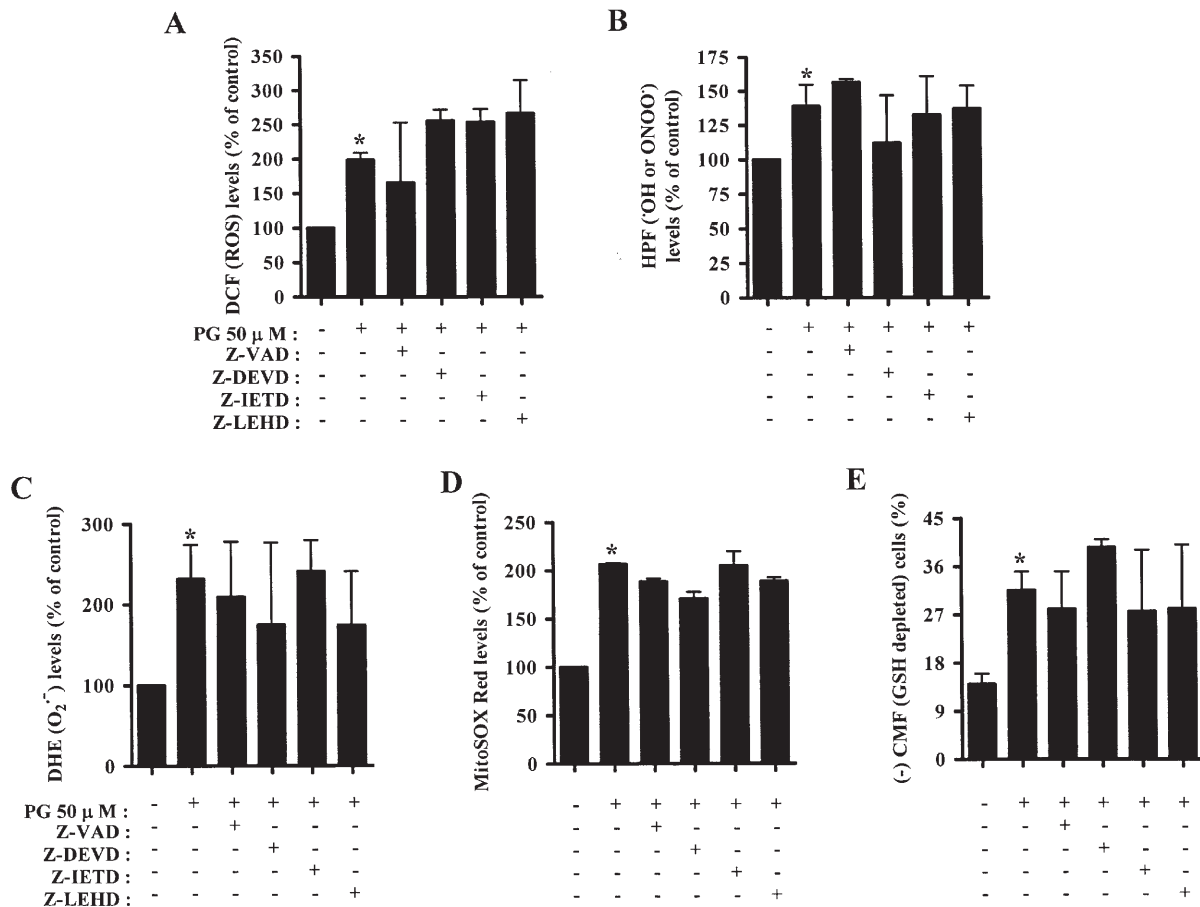


Figure 2. Effects of caspase inhibitors on ROS and GSH levels in PG-treated Calu-6 cells. Exponentially growing cells were treated with 50  $\mu$ M PG for 24 h following 1-h pre-incubation with 12.5  $\mu$ M caspase inhibitor. ROS and GSH levels in Calu-6 cells were measured using a FACStar flow cytometer. (A) DCF (ROS) levels. (B) HPF (OH or ONOO<sup>-</sup>) levels. (C) DHE (O<sub>2</sub><sup>-</sup>) levels. (D) MitoSox (mitochondrial O<sub>2</sub><sup>-</sup>) levels. (E) The percentage of GSH-depleted (CMF-negative) cells. \*P<0.05 compared with the PG-untreated control group.

of intracellular ROS in PG-treated Calu-6 cells were altered by treatment with each inhibitor of caspase, we assessed the levels of intracellular ROS and GSH in Calu-6 cells by using various fluorescence dyes at 24 h. As shown in Fig. 2A and B, intracellular general ROS levels such as H<sub>2</sub>O<sub>2</sub>, OH and ONOO<sup>-</sup> were increased in 50  $\mu$ M PG-treated cells. Treatment with caspase inhibitors did not significantly alter the ROS levels in PG-treated cells. When we detected the intracellular O<sub>2</sub><sup>-</sup> levels in PG-treated Calu-6 cells, red fluorescence derived from DHE reflecting intracellular O<sub>2</sub><sup>-</sup> levels and MitoSox reflecting mitochondrial O<sub>2</sub><sup>-</sup> levels was significantly increased in these cells at 24 h (Fig. 2C and D). None of the caspase inhibitors significantly altered the intracellular or mitochondrial O<sub>2</sub><sup>-</sup> levels in PG-treated Calu-6 cells (Fig. 2C and D).

Cellular GSH has been shown to be crucial for regulation of cell proliferation, cell cycle progression and apoptosis (28,29). Therefore, we analyzed the changes in GSH levels in Calu-6 cells by using CMF fluorescence at 24 h. As shown in Fig. 2E, treatment with PG depleted the intracellular GSH content in Calu-6 cells, and none of the caspase inhibitors prevented the depletion of GSH content in PG-treated Calu-6 cells. Caspase inhibitors alone did not significantly change the levels of ROS and GSH in Calu-6 control cells at 24 h (data not shown).

*Effects of caspase inhibitors on ROS and GSH levels in PG-treated Calu-6 cells at 72 h.* Since caspase inhibitors showing an anti-apoptotic effect on PG-treated Calu-6 cells did not significantly change the ROS and GSH levels at 24 h, we evaluated the changes in these cells at the late time of 72 h. Treatment with pan-caspase inhibitor, Z-VAD, significantly decreased the levels of apoptosis in PG-treated cells as observed at 24 h (Fig. 3A). Z-VAD also decreased the MMP loss in these cells (Fig. 3B). In contrast to ROS levels in PG-treated Calu-6 cells at 24 h, PG did not increase but decreased the ROS levels in Calu-6 control cells at 72 h (Fig. 3C). Z-VAD slightly increased the ROS levels in PG-treated cells (Fig. 3C). The intracellular O<sub>2</sub><sup>-</sup> level was increased in Calu-6 cells at 72 h, and Z-VAD did not change the O<sub>2</sub><sup>-</sup> levels in PG-treated cells (Fig. 3D).

In relation to GSH levels in PG-treated cells at 72 h, the depletion levels of GSH in these cells were slightly higher than those at 24 h (Fig. 4A). Notably, treatment with Z-VAD significantly reduced the depletion of GSH content in PG-treated cells at 72 h (Fig. 4A). Next, to evaluate whether the M1 region cells (Fig. 4A) were dead or not, we stained cells with PI additionally to verify disruption of the plasma membrane. As shown in Fig. 4B, many negative CMF fluorescence cells by PG showed PI-positive staining, which indicated that many cells showing GSH depletion were

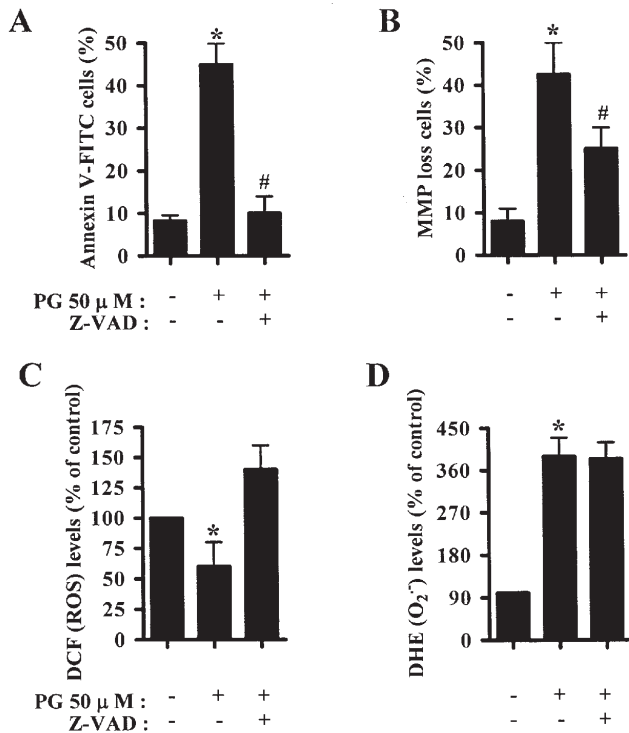


Figure 3. Effects of Z-VAD on apoptosis, MMP loss and ROS levels in PG-treated Calu-6 cells. Exponentially growing cells were treated with 50  $\mu$ M PG for 72 h following 1-h pre-incubation with 12.5  $\mu$ M Z-VAD. (A) Percentages of Annexin V-positive cells. (B) Rhodamine 123-negative (MMP loss) cells. (C) Levels of DCF (ROS). (D) Levels of DHE ( $O_2^{\cdot-}$ ). \*P<0.05 compared with the PG-untreated control group; #P<0.05 compared with cells treated with only PG.

considered to be dead. The treatment of Z-VAD significantly reduced the number of CMF negative and PI-positive cells in PG-treated cells. The proportion of CMF and PI-double-positive cells was small; ~4% in control and PG-treated cells (Fig. 4B). Caspase inhibitors alone did not significantly change the levels of apoptosis, ROS and GSH in Calu-6 control cells at 72 h (data not shown).

## Discussion

In the present study, we focused on evaluating the anti-apoptotic effects of caspase inhibitors (pan-caspase, caspase-3, -8 or -9) in relation to changes in ROS and GSH levels in PG-treated human pulmonary adenocarcinoma Calu-6 cells, since we previously observed that PG inhibited the growth of Calu-6 cells via apoptosis (unpublished data). Treatment with each tested caspase inhibitor significantly prevented apoptosis in PG-treated Calu-6 cells at 24 h (Fig. 1B). The anti-apoptotic effects of caspase inhibitors (caspase-3, -8 or -9) on these cells were also observed at 72 h (data not shown). These data suggest that the activation of caspase-3, -8 and -9 together is necessary for full induction of apoptosis. The modes of caspase activation during apoptosis by PG may be dependent on cell type. For example, although there were differences in the incubation time and concentration of caspase inhibitors, caspase inhibitors were ineffective for rescuing cells from PG-induced apoptosis in pheochromocytoma PC12 (8), As4.1 juxtaglomerular (30) and HeLa cells (31). In particular, the inhibitor of caspase-8 decreased the levels of apoptosis in PG-treated Calu-6 cells. The exact mechanism of PG

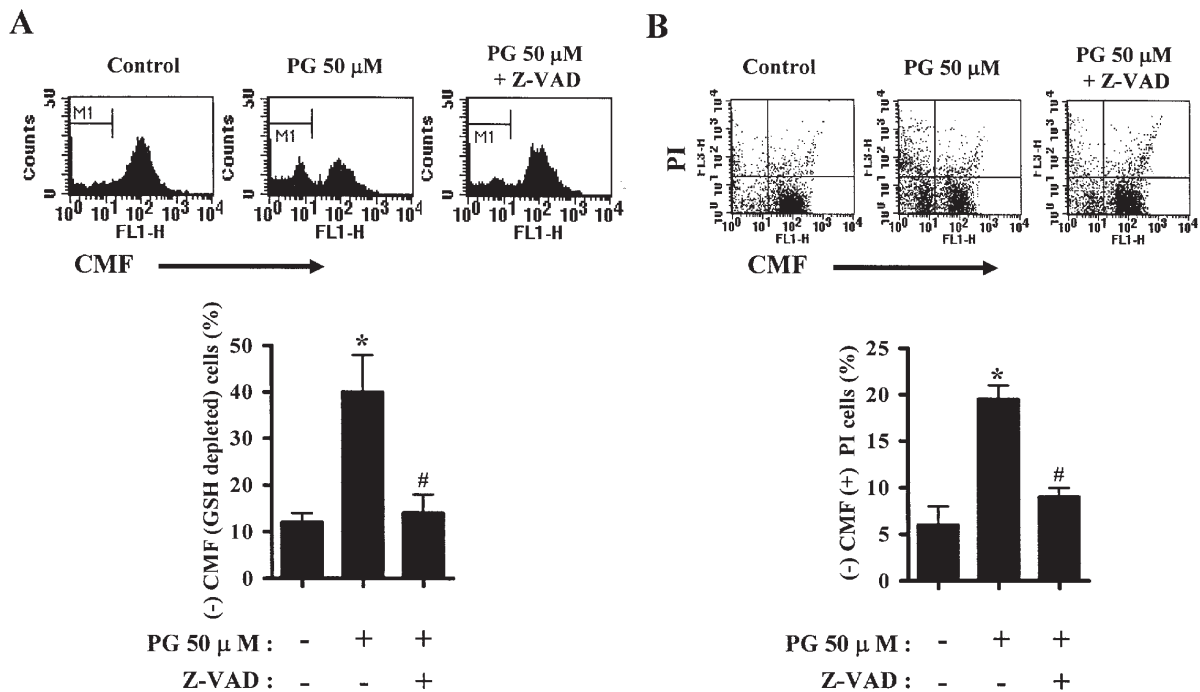


Figure 4. Effects of Z-VAD on GSH content and membrane integrity in PG-treated Calu-6 cells. Exponentially growing cells were treated with 12.5  $\mu$ M PG for 72 h following 1-h pre-incubation with 12.5  $\mu$ M Z-VAD. (A) The intracellular GSH levels were determined by a FACStar flow cytometer. The graph shows the percent of CMF-negative fluorescent (GSH depleted; M1 region) cells from the above figures. (B) CMF fluorescent cells and PI-positive stained cells were also measured using a FACStar flow cytometer. The graph shows the percent of CMF-negative and PI-positive stained cells from the above figures. \*P<0.05 compared with the PG-untreated control group; #P<0.05 compared with cells treated with only PG.

activation of caspase-8 requires further study, since the activation of caspase-8 is related to the cell death receptor pathway in apoptosis (2,3). With regard to the MMP loss ( $\Delta\Psi_m$ ), the loss of MMP ( $\Delta\Psi_m$ ) was observed in PG-treated cells at 24 or 72 h. Each inhibitor of caspase did not recover the loss of MMP ( $\Delta\Psi_m$ ) in PG-treated cells at 24 h, which suggests that the loss of MMP ( $\Delta\Psi_m$ ) by PG was not enough to completely induce apoptosis in Calu-6 cells at this time point. However, we observed that Z-VAD in part prevented the loss of MMP ( $\Delta\Psi_m$ ) at 72 h. This result also suggests that other pathways including the cell death receptor pathway, in addition to the loss of MMP ( $\Delta\Psi_m$ ) by PG, is required to entirely trigger apoptosis.

PG can disturb the natural oxidation and reduction equilibrium in cells. It has been reported that an increased pattern of  $O_2^-$  by PG is shown in pheochromocytoma PC12 (8), human neuroblastoma SH-SY5Y (32) and As4.1 juxtaglomerular cells (21). Likewise, our data showed that the intracellular ROS levels as well as  $O_2^-$  levels were increased in 50  $\mu$ M PG-treated Calu-6 cells at 24 h. However, treatment with 50  $\mu$ M PG decreased the ROS levels such as  $H_2O_2$ , OH and ONOO for the long incubation time of 72 h. It is possible that PG decreased SOD activity, resulting in slow conversion from  $O_2^-$  to  $H_2O_2$ , reduction in  $H_2O_2$  levels, and accumulation of  $O_2^-$ . In fact, we recently reported that PG decreases the activity of SOD (33). All of the tested caspase inhibitors, which significantly prevented cell death, did not significantly decrease the ROS levels increased by PG. None of the caspase inhibitors decreased the  $O_2^-$  levels in PG-treated Calu-6 cells as well. Our results suggest that the changes in ROS by PG are not tightly related to apoptosis induction in Calu-6 cells. The exact mechanisms of cell death due to PG and the roles of ROS in PG-treated Calu-6 cells still need to be defined further.

GSH is a main non-protein antioxidant in cells. It is able to clear away  $O_2^-$  and provide electrons for enzymes such as glutathione peroxidase, which reduce  $H_2O_2$  to  $H_2O$ . It has been reported that the intracellular GSH content has a decisive effect on anticancer drug-induced apoptosis, indicating that apoptotic effects are inversely correlated to GSH content (21,34,35). Likewise, our results clearly indicate that PG depleted intracellular GSH content in Calu-6 cells. In fact, Z-VAD showing an anti-apoptotic effect on PG-treated Calu-6 cells reduced the depletion of GSH content by PG at 72 h. Many CMF-negative fluorescent cells induced by PG also showed PI-positive staining, which indicated that many cells showing GSH depletion were considered to be dead. The treatment of Z-VAD significantly reduced the number of CMF-negative and PI-positive cells in PG-treated cells, indicating that Z-VAD keeps the integrity of the plasma membrane in PG-treated cells. These results suggest that intracellular GSH levels are tightly related to PG-induced cell death. However, notably, Z-VAD did not decrease the depletion of GSH content by PG at 24 h. These data suggest that the depletion of GSH by PG at 24 h was not dependent on the activation of caspase but the depletion of GSH at the late time phase of 72 h was.

In conclusion, PG inhibited the growth of Calu-6 cells throughout caspase-dependent apoptosis. The anti-apoptotic effect of caspase inhibitors on PG-induced Calu-6 cell death

was closely related to the changes in GSH content rather than ROS levels.

## Acknowledgements

This research was supported by the Korean Science and Engineering Foundation (grant no. R01-2006-000-10544-0) and a Korea Research Foundation Grant funded by the Government of the Republic of Korea (MOEHRD).

## References

- Shi Y: Mechanisms of caspase activation and inhibition during apoptosis. *Mol Cell* 9: 459-470, 2002.
- Ashkenazi A and Dixit VM: Death receptors: signaling and modulation. *Science* 281: 1305-1308, 1998.
- Budihardjo I, Oliver H, Lutter M, Luo X and Wang X: Biochemical pathways of caspase activation during apoptosis. *Annu Rev Cell Dev Biol* 15: 269-290, 1999.
- Mehmet H: Caspases find a new place to hide. *Nature* 403: 29-30, 2000.
- Hengartner MO: The biochemistry of apoptosis. *Nature* 407: 770-776, 2000.
- Liu X, Yue P, Zhou Z, Khuri FR and Sun SY: Death receptor regulation and celecoxib-induced apoptosis in human lung cancer cells. *J Natl Cancer Inst* 96: 1769-1780, 2004.
- Saeki K, Hayakawa S, Isemura M and Miyase T: Importance of a pyrogallol-type structure in catechin compounds for apoptosis-inducing activity. *Phytochemistry* 53: 391-394, 2000.
- Yamada J, Yoshimura S, Yamakawa H, *et al*: Cell permeable ROS scavengers, Tiron and Tempol, rescue PC12 cell death caused by pyrogallol or hypoxia/reoxygenation. *Neurosci Res* 45: 1-8, 2003.
- Gonzalez C, Sanz-Alfayate G, Agapito MT, Gomez-Nino A, Rocher A and Obeso A: Significance of ROS in oxygen sensing in cell systems with sensitivity to physiological hypoxia. *Respir Physiol Neurobiol* 132: 17-41, 2002.
- Baran CP, Zeigler MM, Tridandapani S and Marsh CB: The role of ROS and RNS in regulating life and death of blood monocytes. *Curr Pharm Des* 10: 855-866, 2004.
- Bubici C, Papa S, Pham CG, Zazzeroni F and Franzoso G: The NF-kappaB-mediated control of ROS and JNK signaling. *Histol Histopathol* 21: 69-80, 2006.
- Zorov DB, Juhaszova M and Sollott SJ: Mitochondrial ROS-induced ROS release: An update and review. *Biochim Biophys Acta* 1757: 509-517, 2006.
- Zelko IN, Mariani TJ and Folz RJ: Superoxide dismutase multigene family: a comparison of the CuZn-SOD (SOD1), Mn-SOD (SOD2), and EC-SOD (SOD3) gene structures, evolution, and expression. *Free Radic Biol Med* 33: 337-349, 2002.
- Wilcox CS: Reactive oxygen species: roles in blood pressure and kidney function. *Curr Hypertens Rep* 4: 160-166, 2002.
- Chen TJ, Jeng JY, Lin CW, Wu CY and Chen YC: Quercetin inhibition of ROS-dependent and -independent apoptosis in rat glioma C6 cells. *Toxicology* 223: 113-126, 2006.
- Dasmahapatra G, Rahmani M, Dent P and Grant S: The typhostin adaphostin interacts synergistically with proteasome inhibitors to induce apoptosis in human leukemia cells through a reactive oxygen species (ROS)-dependent mechanism. *Blood* 107: 232-240, 2006.
- Wallach-Dayana SB, Izbicki G, Cohen PY, Gerstl-Golan R, Fine A and Breuer R: Bleomycin initiates apoptosis of lung epithelial cells by ROS but not by Fas/FasL pathway. *Am J Physiol Lung Cell Mol Physiol* 290: L790-L796, 2006.
- Simon HU, Haj-Yehia A and Levi-Schaffer F: Role of reactive oxygen species (ROS) in apoptosis induction. *Apoptosis* 5: 415-418, 2000.
- Moreno-Manzano V, Ishikawa Y, Lucio-Cazana J and Kitamura M: Selective involvement of superoxide anion, but not downstream compounds hydrogen peroxide and peroxynitrite, in tumor necrosis factor-alpha-induced apoptosis of rat mesangial cells. *J Biol Chem* 275: 12684-12691, 2000.
- Sawada M, Nakashima S, Kiyono T, *et al*: p53 regulates ceramide formation by neutral sphingomyelinase through reactive oxygen species in human glioma cells. *Oncogene* 20: 1368-1378, 2001.

21. Park WH, Han YW, Kim SH and Kim SZ: A superoxide anion generator, pyrogallol induces apoptosis in As4.1 cells through the depletion of intracellular GSH content. *Mutat Res* 619: 81-92, 2007.
22. Petty RD, Nicolson MC, Kerr KM, Collie-Duguid E and Murray GI: Gene expression profiling in non-small cell lung cancer: from molecular mechanisms to clinical application. *Clin Cancer Res* 10: 3237-3248, 2004.
23. Park WH, Seol JG, Kim ES, *et al*: Arsenic trioxide-mediated growth inhibition in MC/CAR myeloma cells via cell cycle arrest in association with induction of cyclin-dependent kinase inhibitor, p21, and apoptosis. *Cancer Res* 60: 3065-3071, 2000.
24. Setsukinai K, Urano Y, Kakinuma K, Majima HJ and Nagano T: Development of novel fluorescence probes that can reliably detect reactive oxygen species and distinguish specific species. *J Biol Chem* 278: 3170-3175, 2003.
25. Macho A, Hirsch T, Marzo I, *et al*: Glutathione depletion is an early and calcium elevation is a late event of thymocyte apoptosis. *J Immunol* 158: 4612-4619, 1997.
26. Hedley DW and Chow S: Evaluation of methods for measuring cellular glutathione content using flow cytometry. *Cytometry* 15: 349-358, 1994.
27. Yang J, Liu X, Bhalla K, *et al*: Prevention of apoptosis by Bcl-2: release of cytochrome c from mitochondria blocked. *Science* 275: 1129-1132, 1997.
28. Poot M, Teubert H, Rabinovitch PS and Kavanagh TJ: De novo synthesis of glutathione is required for both entry into and progression through the cell cycle. *J Cell Physiol* 163: 555-560, 1995.
29. Schnelldorfer T, Gansauge S, Gansauge F, Schlosser S, Beger HG and Nussler AK: Glutathione depletion causes cell growth inhibition and enhanced apoptosis in pancreatic cancer cells. *Cancer* 89: 1440-1447, 2000.
30. Park WH, Han YH, Kim SH and Kim SZ: Pyrogallol, ROS generator inhibits As4.1 juxtaglomerular cells via cell cycle arrest of G2 phase and apoptosis. *Toxicology* 235: 130-139, 2007.
31. Kim SW, Han YW, Lee ST, *et al*: A superoxide anion generator, pyrogallol, inhibits the growth of HeLa cells via cell cycle arrest and apoptosis. *Mol Carcinog* 47: 114-125, 2007.
32. Poulouse SM, Harris ED and Patil BS: Citrus limonoids induce apoptosis in human neuroblastoma cells and have radical scavenging activity. *J Nutr* 135: 870-877, 2005.
33. Han YH, Kim SZ, Kim SH and Park WH: Apoptosis in pyrogallol-treated Calu-6 cells is correlated with the changes of intracellular GSH levels rather than ROS levels. *Lung Cancer* 59: 301-314, 2008.
34. Estrela JM, Ortega A and Obrador E: Glutathione in cancer biology and therapy. *Crit Rev Clin Lab Sci* 43: 143-181, 2006.
35. Higuchi Y: Glutathione depletion-induced chromosomal DNA fragmentation associated with apoptosis and necrosis. *J Cell Mol Med* 8: 455-464, 2004.